

Observations of Al segregation around dislocations in AlGaN

L. Chang, S. K. Lai, F. R. Chen, and J. J. Kai

Citation: *Applied Physics Letters* **79**, 928 (2001); doi: 10.1063/1.1391409

View online: <http://dx.doi.org/10.1063/1.1391409>

View Table of Contents: <http://scitation.aip.org/content/aip/journal/apl/79/7?ver=pdfcov>

Published by the [AIP Publishing](#)

Articles you may be interested in

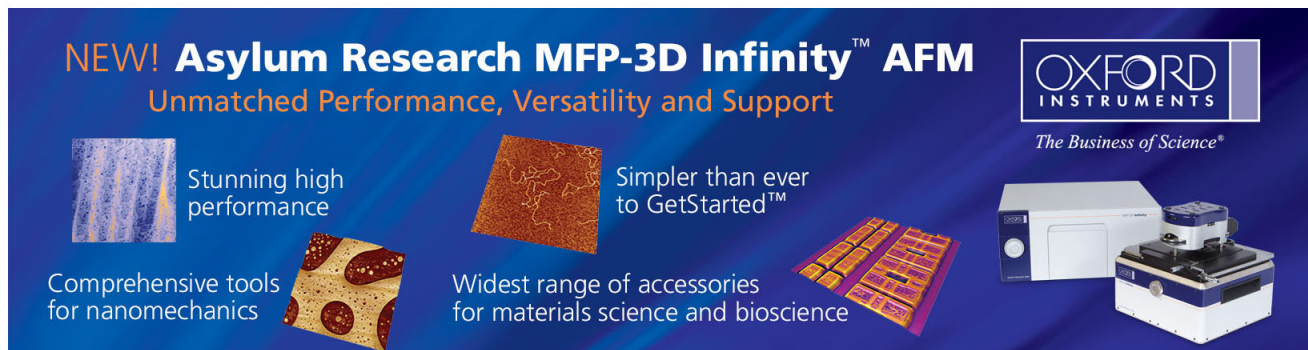
[Dislocation blocking by AlGaN hot electron injecting layer in the epitaxial growth of GaN terahertz Gunn diode](#)
J. Appl. Phys. **114**, 104508 (2013); 10.1063/1.4820460

[High conductive gate leakage current channels induced by In segregation around screw- and mixed-type threading dislocations in lattice-matched In_xAl_{1-x}N / GaN heterostructures](#)
Appl. Phys. Lett. **97**, 232106 (2010); 10.1063/1.3525713

[Influence of alloy composition and interlayer thickness on twist and tilt mosaic in Al_xGa_{1-x}N/AlN/GaN heterostructures](#)
Appl. Phys. Lett. **83**, 5434 (2003); 10.1063/1.1637717

[Dislocation annihilation by silicon delta-doping in GaN epitaxy on Si](#)
Appl. Phys. Lett. **81**, 4712 (2002); 10.1063/1.1529309

[Observation of coreless edge and mixed dislocations in Mg-doped Al_{0.03}Ga_{0.97}N](#)
Appl. Phys. Lett. **81**, 4541 (2002); 10.1063/1.1527978

The advertisement features a dark blue background with white and orange text. At the top left, it reads 'NEW! Asylum Research MFP-3D Infinity™ AFM' in large white letters, followed by 'Unmatched Performance, Versatility and Support' in orange. To the right is the Oxford Instruments logo, which includes the text 'OXFORD INSTRUMENTS' and the tagline 'The Business of Science®'. Below the text are four images: a textured surface, a circular pattern, a grid of small squares, and the physical AFM instrument. Each image is accompanied by a short text description: 'Stunning high performance', 'Simpler than ever to GetStarted™', 'Comprehensive tools for nanomechanics', and 'Widest range of accessories for materials science and bioscience'.

Observations of Al segregation around dislocations in AlGaN

L. Chang^{a)}

Department of Materials Science and Engineering, National Chiao Tung University, Hsinchu, Taiwan

S. K. Lai, F. R. Chen, and J. J. Kai

Department of Engineering and System Science, National Tsing Hua University, Hsinchu, Taiwan

(Received 16 March 2001; accepted for publication 11 June 2001)

Transmission electron microscopy has been used to observe Al segregation around the threading dislocations in $\text{Al}_{0.1}\text{Ga}_{0.9}\text{N}$ and $\text{Al}_{0.3}\text{Ga}_{0.7}\text{N}$ grown by metalorganic chemical vapor deposition on 6H-SiC. Dislocation lines were found to have up to 70% more Al concentration than those regions free of dislocations in the matrix. The Al-depleted regions around the dislocations are shown to be within a few nanometers from the dislocation lines. The results also show that more Al segregate to edge dislocations than to screw ones. © 2001 American Institute of Physics.

[DOI: 10.1063/1.1391409]

GaN is a wide band gap material and has many excellent properties for optical and electronic applications. $\text{Al}_x\text{Ga}_{1-x}\text{N}$ ($x \sim 0.1-0.3$) has been often used as the cladding layer or quantum well layer in GaN-related devices of blue light-emitting diodes, laser diodes, and power transistors.^{1,2} The microstructures of AlGaN have been a subject of intensive research for the past few years.²⁻⁴ AlGaN grown on sapphire or SiC substrate often contains a large number of dislocations (dislocation density $\sim 10^9/\text{cm}^2$) due to the lattice mismatch. A lower density of dislocations is a necessary condition for high quality GaN films as the dislocations degrade the optoelectronic properties. Most of the works on GaN-related materials in the past have focused on the structural characteristics of dislocations and their effects on the optoelectronic properties.⁵⁻⁷ However, little attention has been paid to the composition variations within AlGaN ternary alloys. In this letter, we present evidence of Al segregation around the dislocations in AlGaN alloys based on the observations of transmission electron microscopy (TEM) with x-ray energy dispersive spectroscopy (EDX) and electron energy loss spectroscopy (EELS) with a spatial resolution of nanometer.⁸

Heteroepitaxial AlGaN films in two different compositions were grown on 6H-SiC (0001) by metalorganic chemical vapor deposition (MOCVD). The nominal concentrations of Al and Ga were deduced from x-ray diffraction to be $\text{Al}_{0.1}\text{Ga}_{0.9}\text{N}$ and $\text{Al}_{0.3}\text{Ga}_{0.7}\text{N}$. All the AlGaN films were doped with Si in the order of $10^{18}/\text{cm}^3$. The deposition temperatures were in the range of 1050 °C–1150 °C. The source materials used were triethylaluminum, triethylgallium, and NH_3 . The cross sectional TEM specimens were prepared by a conventional sandwiched method consisting of gluing, mechanical thinning, and ion milling by Ar ion beam to perforation. TEM observations were carried out in a JEOL JEM 2010F microscope with a field-emission gun which can form an electron probe in a 0.5 nm diameter size. The operating voltage was set at 200 kV. The compositions were obtained by EDX from an Oxford Instrument EDX detector with an

ultrathin window and EELS from a Gatan energy filter. All necessary precautions for quantitative analysis of compositions had been taken before the acquisition of the spectra.^{8,9} The compositional measurements were taken from regions with thickness less than 20 nm where high-resolution TEM images could be revealed, so that the thin-film criterion for quantitative analysis is satisfied without the need for correction of the absorption effect. The beam broadening size is estimated to be less than 2 nm. The orientations of the specimens during the EDX acquisition were far from the zone axes and two-beam directions to avoid any significant channeling and absorption effect. The concentrations were determined by assuming that the nitrogen fraction is constant, and the sum of Ga and Al are 100% in total. The intensities of Al *K* and Ga *K* lines, and the calculated *k* factor provided by the program of quantitative analysis of EDX are used for composition determination. The statistic error of each averaged composition is determined at the 99% confidence level by using *t* distribution.

Typical bright-field TEM images of $\text{Al}_{0.1}\text{Ga}_{0.9}\text{N}$ and $\text{Al}_{0.3}\text{Ga}_{0.7}\text{N}$ samples with the incident beam near a $[1\bar{1}00]$ zone axis are shown in Fig. 1. The dislocations grown from

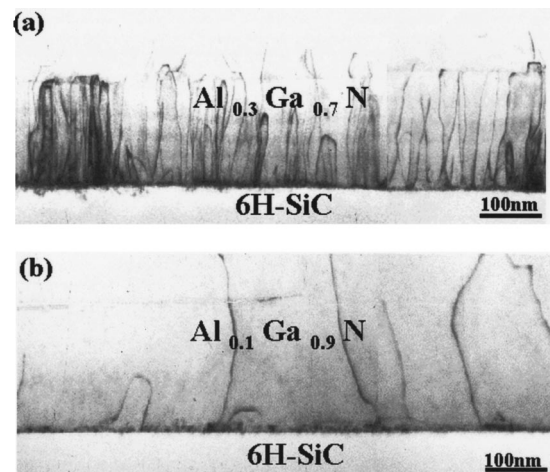


FIG. 1. Bright-field TEM micrographs showing dislocations in (a) $\text{Al}_{0.3}\text{Ga}_{0.7}\text{N}$ and (b) $\text{Al}_{0.1}\text{Ga}_{0.9}\text{N}$ are shown.

^{a)}Author to whom correspondence should be addressed; electronic mail: lichang@cc.nctu.edu.tw

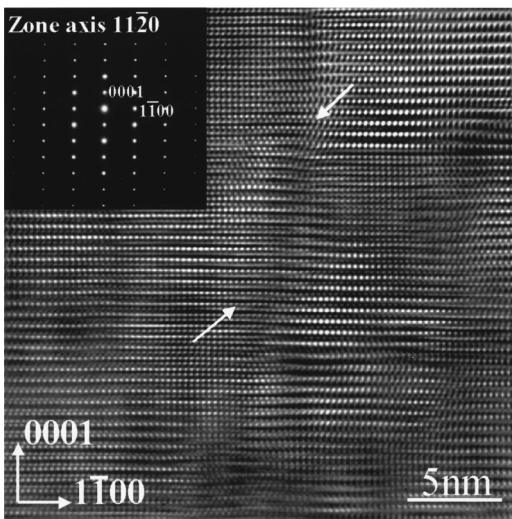


FIG. 2. High-resolution TEM image showing partial dislocations as arrowed is shown.

the interface between AlGa_{0.3}N and SiC are clearly seen. The dislocation density of Al_{0.1}Ga_{0.9}N is estimated in the range of 10^9 cm^{-2} , and the mean dislocation spacing is about 300 nm. For the Al_{0.3}Ga_{0.7}N samples, the dislocation density is of the order of 10^{10} cm^{-2} with the mean dislocation spacing of about 40 nm. These threading dislocations grown in the AlGa_{0.3}N layer are originated from the interface with SiC during MOCVD deposition due to the lattice misfit between AlGa_{0.3}N and SiC. The conventional $\mathbf{g} \cdot \mathbf{b}$ invisibility criterion (where \mathbf{g} is the reflection vector used for imaging a dislocation with Burger's vector \mathbf{b}) was used to determine the dislocation type and the Burger's vectors. The edge type dislocations have the Burger's vector $1/3 \langle 11\bar{2}0 \rangle$, the screw $[0001]$, and the mixed $1/3 \langle 11\bar{2}3 \rangle$. Detailed examination of the diffraction patterns confirms that no precipitate and/or phase separation exist in the AlGa_{0.3}N layer. A high-resolution TEM image in Fig. 2 also shows partial dislocations without the presence of second phase. Thus, it is certain that the dark line of contrast in the TEM images is mainly due to the strain field of a dislocation in the AlGa_{0.3}N layer. Dark-field imaging by the weak beam technique also confirms this point.

EDX from areas probed by a micron-size electron beam on Al_{0.3}Ga_{0.7}N samples shows that the averaged Al concentration is $29.0 \pm 2.0 \text{ at} \%$ close to the nominal value of 30%. However, nanobeam measurements show that the matrix free of dislocations has only $21.0 \pm 1.2 \text{ at} \%$ Al. The EDX spectra from an edge dislocation and a region in the matrix free of dislocations in Al_{0.3}Ga_{0.7}N, acquired at the same electron beam condition, are superimposed as shown in Fig. 3(a). These spectra were obtained in the Al_{0.3}Ga_{0.7}N layer at a distance of more than 60 nm away from the interface between AlGa_{0.3}N and SiC. With normalization of the intensities in these two spectra with respect to the Ga *K* lines which have been adjusted to the same height, it is obvious that the Al intensity is much higher at the dislocation. The Al concentration is $36.0 \pm 1.9 \text{ at} \%$ in average at the edge dislocation lines. Compared with the matrix, the dislocation core in Al_{0.3}Ga_{0.7}N can be enriched with more than 70% increase of Al. The Si peak is believed to come from the so-called Si internal fluorescence peak due to the dead layer of the Si(Li) crystal in the EDX detector,¹⁰ and partly from the doping of

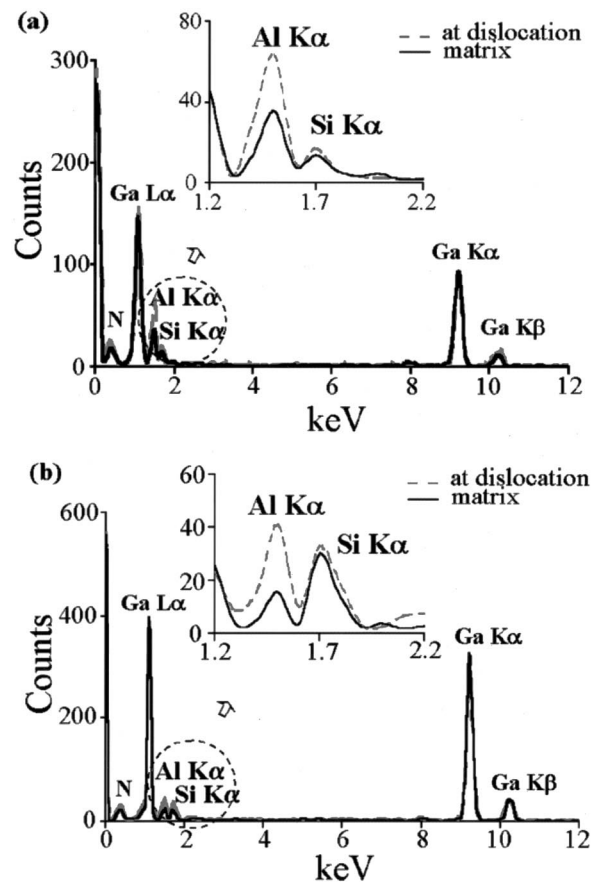


FIG. 3. EDX spectra from an edge dislocation and from the matrix superimposed are shown. Al peaks are enlarged in the inset and (a) Al_{0.3}Ga_{0.7}N and (b) Al_{0.1}Ga_{0.9}N are presented.

Si in deposition. Since the distribution of Si intensity is uniform over the AlGa_{0.3}N layer, the effect on the results can be ignored. For the Al_{0.1}Ga_{0.9}N case, Fig. 3(b) also shows the Al enrichment at an edge dislocation in comparison with the matrix. The matrix contains $9.6 \pm 0.3 \text{ at} \%$ Al, while there exists about $15.6 \pm 1.0 \text{ at} \%$ Al at the edge dislocations. The Al composition profiles across the edge dislocations in both alloys are demonstrated in Fig. 4. It is apparent that Al is enriched around the dislocation cores, but depleted at both sides in 2–3 nm regions. The depletion of Al to 4–6 at % is very significant in Al_{0.1}Ga_{0.9}N, while it is about 15 at % in Al_{0.3}Ga_{0.7}N. It is likely that the Al concentration at the dislocation cores may be much higher than the measured values if the beam broadening effect could be corrected. More than five dislocations characterized in each alloy show the similar profiles. The EELS maps in higher spatial resolution also confirm Al segregation at the dislocations. Measurements at the screw and mixed dislocations indicate that the enriched Al concentration is about 31 and 34 at % in average, respectively, in Al_{0.3}Ga_{0.7}N, whereas it is 12.2 and 13 at % in Al_{0.1}Ga_{0.9}N. The Al segregation at the screw type dislocations is less severe than at the edge type. For the mixed dislocations, it lies between the edge and the screw types. These results show similar behaviors of Al segregation around dislocations in both Al_{0.1}Ga_{0.9}N and Al_{0.3}Ga_{0.7}N alloys.

Solute segregation to dislocations is often observed in metallic alloys, for example, carbon atoms in α -iron can

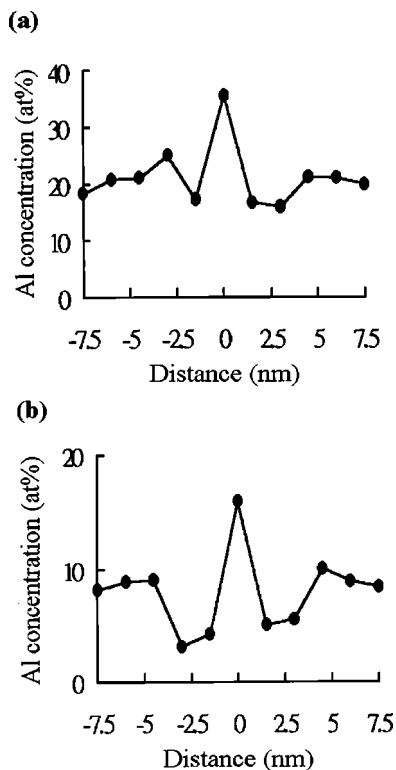


FIG. 4. Typical Al composition profile across an edge dislocations in (a) $\text{Al}_{0.3}\text{Ga}_{0.7}\text{N}$ and (b) $\text{Al}_{0.1}\text{Ga}_{0.9}\text{N}$ is shown.

segregate around dislocations to form the Cottrell atmosphere,^{11–13} and boron segregation in FeAl alloys.¹⁴ In a study of In distribution in InGaN, Sato *et al.* and Duxbury *et al.* reported that In segregation to dislocations occurred.^{15,16} It is known that the Al atom has a smaller size than the Ga. Therefore, Al segregation to the dislocations in AlGaN is reasonable because the strain energy of dislocation can be reduced. The strong enrichment of Al at a dislocation core may imply that an Al atom has a higher interaction energy with a dislocation than Ga. Hence, the reduction of line energy can be done by segregation of Al to dislocations. It has been shown that the edge dislocation in GaN has a higher line energy than the screw.¹⁷ From our EDX results, however, the enrichment of Al at edge dislocations appears much stronger than at screw dislocations. This may imply that the interaction energy of Al atoms with an edge dislocation is greater than with a screw, probably due to the absence of elastic displacements parallel to the basal plane for a screw.¹⁸ In metallic alloys, the concentration of solute segregation is exponentially decreased with the interaction energy which is a function of distance from a dislocation line. In the present case, we have observed Al depletion adjacent to enriched dislocation cores, which is different from the distribution in metallic alloys. The reason about the Al depletion is not clearly known. It might result from deposition during which dislocation formation was accompanied by clustering of more Al atoms. An alternative speculation might be that Al diffusion is very slow in the wurtzite structure with covalent bonding during deposition, so that it can not compensate those segregated to dislocations where they act as sinks for

Al. This can be reasoned as the higher strain energy or the stronger stress field near a dislocation core might accelerate those Al atoms within a few nanometer regions of the dislocation to migrate to the core. Further experiments of high temperature annealing for long periods are undertaken to clarify the mechanism. Also, we still need to quantitatively evaluate the segregation effect on optoelectronic properties. The presence of Al segregation around dislocations may pin the dislocation lines, resulting in difficulty of movement. As the consequence, the dislocation density may not be easily reduced. Thus, the process modification is necessary if a low dislocation density is desired for the AlGaN layer.

In summary, Al segregation around the dislocations in AlGaN alloys grown on 6H-SiC has been observed by TEM. The Al concentration enriched at the dislocation core can be more than 1.6 times as high as that in the matrix. The Al-enriched level depends on the dislocation type, which the strongest is around the edge type, the next is around the mixed type, and the weakest is around the screw type. Also, Al-depleted regions surrounded the enriched dislocation cores have been revealed to be a few nanometers away.

The authors are grateful to EpiStar Corporation, Taiwan, for providing the AlGaN samples.

- ¹O. Ambacher, *J. Phys. D* **31**, 2653 (1998).
- ²J. A. Smart, A. T. Schremer, N. G. Weimann, O. Ambacher, L. F. Eastman, and J. R. Shealy, *Appl. Phys. Lett.* **75**, 388 (1999).
- ³M. D. Bremser, W. G. Perry, T. Zheleva, N. V. Edwards, O. H. Nam, N. Parikh, D. E. Aspnes, and R. F. Davis, *MRS Internet J. Nitride Semicond. Res.* **1**, 8 (1996).
- ⁴G. Steude, T. Christmann, B. K. Meyer, A. Goeldner, A. Hoffmann, F. Bertram, J. Christen, H. Amano, and I. Akasaki, *MRS Internet J. Nitride Semicond. Res.* **4S1**, G3.26 (1999).
- ⁵F. A. Ponce, D. Cherns, W. T. Young, and J. W. Steeds, *Appl. Phys. Lett.* **69**, 770 (1996).
- ⁶Y. Xin, S. J. Pennycook, N. D. Browning, P. D. Nelist, S. Sivanthana, F. Omnes, B. Beaumont, J.-P. Faurie, and P. Gibart, *Appl. Phys. Lett.* **72**, 2680 (1998).
- ⁷J. S. Speck and S. J. Rosner, *Physica B* **274**, 24 (1999).
- ⁸R. F. Egerton, *Electron Energy-Loss Spectroscopy in the Electron Microscope*, 2nd ed. (Plenum, New York, 1996).
- ⁹J. I. Goldstein, D. B. Williams, and G. Cliff, in *Principles of Analytical Electron Microscopy*, edited by D. C. Joy, A. D. Romig, Jr., and J. I. Goldstein (Plenum, New York, 1986), pp. 155–217.
- ¹⁰D. E. Newbury, in *X-Ray Spectrometry in Electron Beam Instruments*, edited by D. B. Williams, J. I. Goldstein, and D. E. Newbury (Plenum, New York, 1995), p. 179.
- ¹¹A. H. Cottrell and B. A. Billy, *Proc. Phys. Soc., London, Sect. A* **62**, 49 (1949).
- ¹²L. Chang, S. J. Barnard, G. D. W. Smith, in *Fundamentals of Aging and Tempering in Bainitic and Martensitic Steel Products*, edited by G. Klause and P. E. Repas (Iron & Steel Society, Warrendale, PA, 1992), pp. 19–28.
- ¹³J. Wilde, A. Cerezo, and G. D. W. Smith, *Scr. Mater.* **43**, 39 (2000).
- ¹⁴D. Blavette, E. Dadel, A. Fraczkiewicz, and A. Menand, *Science* **286**, 2317 (1999).
- ¹⁵H. Sato, T. Sugahara, Y. Naoi, and S. Sakai, *Jpn. J. Appl. Phys., Part 1* **37**, 2013 (1998).
- ¹⁶N. Duxbury, U. Bangert, P. Dawson, E. J. Thrush, W. Van der Stricht, K. Jacobs, and I. Moerman, *Appl. Phys. Lett.* **76**, 1600 (2000).
- ¹⁷J. Elsner, R. Jones, P. K. Sitch, V. D. Porezag, M. Elstner, T. Frauenheim, M. I. Heggie, S. Oberg, and P. R. Briddon, *Phys. Rev. Lett.* **79**, 3672 (1997).
- ¹⁸X. H. Wu, L. M. Brown, D. Kapolnek, S. Keller, B. Keller, S. P. DenBaars, and J. S. Speck, *J. Appl. Phys.* **80**, 3228 (1996).